World Academy of Science, Engineering and Technology
International Journal of Electrical and Computer Engineering
Vol:8, No:11, 2014

Matrix Converter Fed Brushless DC Motor Using Field Programmable Gate Array

P. Subha Karuvelam, M. Rajaram

***Abstract*—**Brushless DC motors (BLDC) are widely used in industrial areas. The BLDC motors are driven either by indirect AC-AC converters or by direct AC-AC converters. Direct AC-AC converters i.e. matrix converters are used in this paper to drive the three phase BLDC motor and it eliminates the bulky DC link energy storage element. A matrix converter converts the AC power supply to an AC voltage of variable amplitude and variable frequency. A control technique is designed to generate the switching pulses for the three phase matrix converter. For the control of speed of the BLDC motor a separate PI controller and Fuzzy Logic Controller (FLC) are designed and a hysteresis current controller is also designed for the control of motor torque. The control schemes are designed and tested separately. The simulation results of both the schemes are compared and contrasted in this paper. The results show that the fuzzy logic control scheme outperforms the PI control scheme in terms of dynamic performance of the BLDC motor. Simulation results are validated with the experimental results.

***Keywords*—**Fuzzy logic controller, matrix converter, permanent magnet brushless DC motor, PI controller.

I. Introduction

THE Brushless DC Motor has some advantages over the DC motor and Induction motor. Some of them are: high power density, reliability, and simple control, less maintenance, high dynamic response, longer life span, and low noise, absence of mechanical commutator and brushes and better speed-torque characteristics [1]-[3]. The BLDC motors are increasingly used in computer, automotive, aerospace applications etc. The BLDC motor has permanent magnet as rotor, trapezoidal back electromotive force, and rectangular stator current for constant torque [4]. The motor is driven based on the feedback of rotor position obtained at every 60 electrical degrees [1]-[3]. The BLDC motors are generally controlled by PWM based voltage source inverter. Except automobile applications, the predominant control scheme used for the BLDC motor is to convert the available AC source into the required DC which is a two stage conversion (AC-DC and DC-AC) [5]. In this conventional technique, the diode bridge rectifier (AC-DC) produces high harmonics in the input current and also this technique needs an energy storage element in between two stages. Bulky and limited life span capacitors are used as DC link storage element than an inductor, subsequently the efficiency of the overall system is reduced and power quality issues arises. To eliminate these drawbacks, matrix converters are used to drive the motor instead of two stage converters [6].

Matrix converter is a single stage converter but a virtual DC link is obtained by properly chopping the input voltage [7]. Different types of matrix converter topologies their and control strategies are reported in [14]. Matrix converter has limited voltage ratio of 86.6% and high number of power semiconductor devices. The voltage ratio is improved from 0.866 to 0.97 using square wave modulation and 0.92 using trapezoidal wave modulation [20]. The matrix converter can increasingly be used in industrial applications due to the following advantages: bidirectional power flow, increased power/weight and power/volume ratio, low displacement factor etc. [7], [15]-[17]. Several control techniques are proposed to control the matrix converter namely Venturini Algorithm, PWM, Space vector modulation, Space Vector Pulse Width Modulation [4], [5], [8], [16]. These techniques are applicable only for the motors with sinusoidal back EMF such as induction motor and synchronous motors. The BLDC motor has trapezoidal back EMF [8]-[11]. Therefore, these techniques are not applicable for BLDC motor. A new control technique was proposed in [7], [12], [13] to drive the BLDC motor using matrix converter. In [7], [12] the BLDC motor is driven with matrix converter and the control of speed and torque parameters were not considered. Carrier based modulation scheme to drive the BLDC motor with matrix converter is demonstrated in [12]. A five phase BLDC motor fed by single sided matrix converter with hysteresis band control is reported in [13]. The author had not concentrated in speed characteristics. A new technique is proposed to drive the BLDC motor fed matrix converter and speed and torque of the BLDC motor is controlled. A PI controller and fuzzy logic controller are designed separately for speed controller and a hysteresis controller is designed for current controller to improve the speed and torque characteristics. The system is implemented using FPGA processor. In [24], the author developed a new modulation strategy for multi-level matrix converter.

II. Matrix Converters

Fig. 1 shows the circuit diagram of the three phase matrix converter where A, B, C and a, b and c are the three input and output phases respectively. The matrix converter converts fixed three phase AC supply into variable amplitude and variable frequency three phase AC supply. It consists of an array of 3X3 bidirectional switches that gives 512 switching combinations.

P.Subha Karuvelam Author is with the Government College of Engineering, Tirunelveli, 627007, Tamilnadu, India (e-mail: subha@gcetly.ac.in).

Dr. M. Rajaram, Jr., was with Vice Chancellor, Anna University, Chennai, Tamilnadu, India. (e-mail:rajaramgct@rediffmail.com).

The switching function is

$$S_{ij} = 1; closed \quad i = (A, B, C)$$
$$= 0; \ open \quad j = (a, b, c)$$

In matrix converter, the output phases should never be open circuited since the load is inductive in nature, and the input phases should never be short circuited since the converter is driven by voltage source. By considering the constraint, only 27 switching states can be used out of 512 switching combinations [8]-[11].

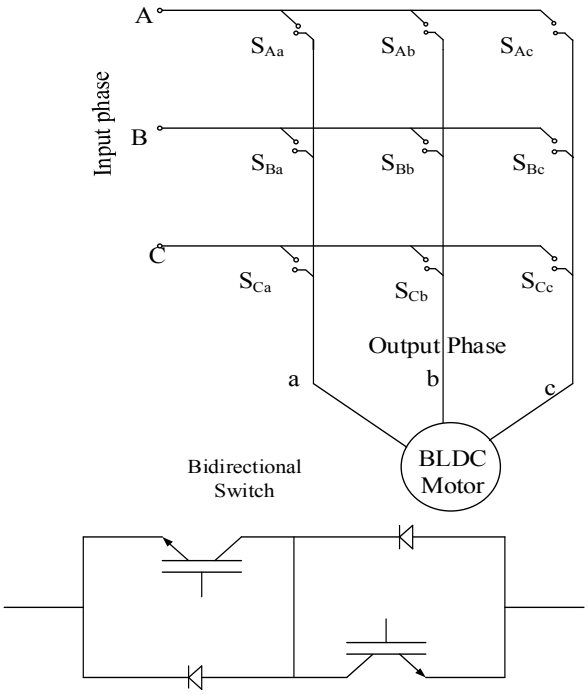

Fig. 1 Circuit diagram of matrix converter

The output phase voltages of the converter are given by

$$\begin{bmatrix} V_a(t) \\ V_b(t) \\ V_c(t) \end{bmatrix} = \begin{bmatrix} S_{Aa}(t) & S_{Ba}(t) & S_{Ca}(t) \\ S_{Ab}(t) & S_{Bb}(t) & S_{Cb}(t) \\ S_{Ac}(t) & S_{Bc}(t) & S_{Cc}(t) \end{bmatrix} \times \begin{bmatrix} V_A(t) \\ V_B(t) \\ V_C(t) \end{bmatrix} \quad (1)$$

$$V_o = S \times V_i$$

where V_o is the output phase voltage, V_i is the input phase voltage and S is switching transfer matrix.

The input phase currents are given by

$$\begin{bmatrix} I_A(t) \\ I_B(t) \\ I_C(t) \end{bmatrix} = \begin{bmatrix} S_{Aa}(t) & S_{Ab}(t) & S_{Ac}(t) \\ S_{Ba}(t) & S_{Bb}(t) & S_{Bc}(t) \\ S_{Ca}(t) & S_{Cb}(t) & S_{Cc}(t) \end{bmatrix} \times \begin{bmatrix} I_a(t) \\ I_b(t) \\ I_c(t) \end{bmatrix} \quad (2)$$

$$I_i = S \times I_o$$

where I_i is the input phase current, I_o is the output phase current and S is switching transfer matrix.

The three phase to three phase matrix converter is formed with nine bidirectional switches. The bidirectional switches are realized by connecting two IGBTs in common collector configuration. Since the IGBTs do not have reverse blocking capability, two fast recovery diodes are connected in antiseries, each in inverse parallel across an IGBT, to sustain the voltage of either polarity when both IGBTs are switched off.

III. Mathematical Modeling of BLDC Motor

The following assumptions are made for simplicity [18], [19], [25]. Stator resistances are equal, self and mutual inductances are constant, semiconductor devices of matrix converter are ideal, armature reaction is ignored, uniform airgap and iron losses are negligible. With these assumptions, the dynamic equations of the BLDC motor can be expresses as

$$\begin{bmatrix} v_a \\ v_b \\ v_c \end{bmatrix} = \begin{bmatrix} R & 0 & 0 \\ 0 & R & 0 \\ 0 & 0 & R \end{bmatrix} \begin{bmatrix} i_a \\ i_b \\ i_c \end{bmatrix} + \begin{bmatrix} L-M & 0 & 0 \\ 0 & L-M & 0 \\ 0 & 0 & L-M \end{bmatrix} \frac{d}{dt} \begin{bmatrix} i_a \\ i_b \\ i_c \end{bmatrix} + \begin{bmatrix} e_a \\ e_b \\ e_c \end{bmatrix} (3)$$

R is the stator resistance; L is the self inductance; M is the mutual inductance; e_a, e_b and e_c are the trapezoidal back EMF.

The trapezoidal back EMF waveforms are modeled as function of rotor position (θ)

$$\begin{bmatrix} e_a \\ e_a \\ e_c \end{bmatrix} = E \begin{bmatrix} f_a(\theta) \\ f_b(\theta) \\ f_c(\theta) \end{bmatrix} \quad (4)$$

where $E = k_e \omega_r$, k_e is the back EMF constant; ω_r is the rotor speed in electrical radians/sec; $f_a(\theta)$, $f_b(\theta)$ and $f_c(\theta)$ are the unity trapezoidal shape function with limit values between +1 and -1 and expressed as

$$f_a(\theta) = \begin{cases} (6/\pi)\theta & (0 < \theta \leq \pi/6) \\ 1 & (\pi/6 < \theta \leq 5\pi/6) \\ -(6/\pi)\theta + 6 & (5\pi/6 < \theta \leq 7\pi/6) \\ -1 & [7\pi/6 < \theta \leq 11\pi/6] \\ (6/\pi)\theta - 12 & (11\pi/6 < \theta \leq 2\pi) \end{cases} \quad (5)$$

$f_b(\theta)$ and $f_c(\theta)$ are determined in the similar way. The electromagnetic torque is expressed as

$$T_e = k_e(f_a(\theta) i_a + f_b(\theta) i_b + f_c(\theta) i_c) \quad (6)$$

The motion equation is expressed as

$$\frac{d\omega_m}{dt} = \left(\frac{P}{2J}\right)(T_e - T_L - B\omega_r) \quad (7)$$

$$\frac{d\theta}{dt} = \omega_r \quad (8)$$

where T_L is the Load Torque in Nm, B is the frictional coefficient in Nms/rad, J is the moment of inertia in kgm^2, P is pole pairs, ω_r is rotor speed in electrical rad/s, ω_m is rotor speed in mechanical rad/s.

IV. Control Principle of Proposed Technique

In indirect transfer function method, the direct matrix converter is considered as virtual rectifier, virtual inverter and virtual DC link. The switching patterns for virtual rectifier and virtual inverter are derived separately.

TABLE I
DETERMINATION OF MAX-MIN VOLTAGES

Angle	Voltage		ON State switches
	Max	Min	
330 - 30°	C	B	S_{C1} and S_{B2}
30 - 90°	A	B	S_{A1} and S_{B2}
90 - 150°	A	C	S_{A1} and S_{C2}
150 - 210°	B	C	S_{B1} and S_{C2}
210 - 270°	B	A	S_{B1} and S_{A2}
270 -330°	C	A	S_{C1} and S_{A2}

A. Realization of DC output – Virtual Rectifier

The two terminal DC output is obtained from the three phase AC using a virtual rectifier. Fig. 2 shows the circuit diagram of the virtual rectifier. In virtual rectifier, among the three input phases, the most positive phase will carry the positive current and most negative phase will carry the negative current. The third phase is inactive phase which carries the zero current. At every moment, the maximum and minimum voltages are sensed. This maximum and minimum voltage changes in every 60 electrical degrees. Table I shows the maximum and minimum voltages over a period of 360°. For example, from 270°-330°, the input phases C and A will be connected with the output phases and so on. The resultant two terminal DC voltage is the envelope of the input voltage.

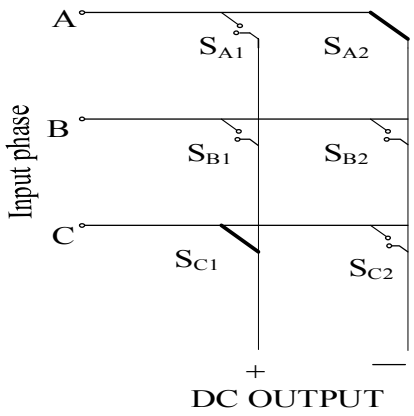

Fig. 2 Virtual rectifier (270°-330°)

B. Realization of Virtual Inverter

Fig. 3 shows the circuit of virtual inverter. The function of the virtual inverter is to excite the BLDC motor stator winding according to the position of the rotor so as to synchronize the stator rotating magnetic field with rotating permanent magnet field. The rotor position of the motor is obtained from three hall sensors.

A single current hall sensor can be used to reconstruct the phase currents of ac motors fed by matrix converter and this method is applicable to only for the motors with sinusoidal back EMF [21]. In [22], instead of hall sensor, a three phase hysteresis comparator is used for commutation of switches and for position sensing. Adaptive flux observer method is used to sense the rotor position and speed in matrix converter fed synchronous machine [23].

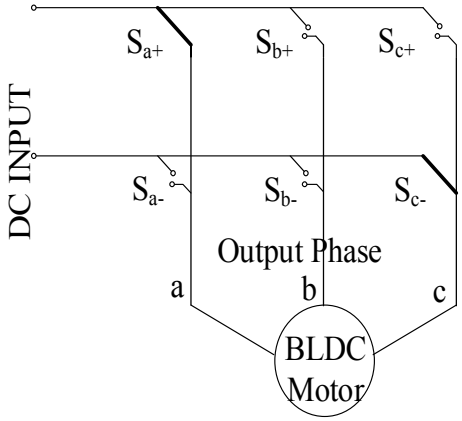

Fig. 3 Virtual inverter (Rotor position is 0 - 60°)

In this paper, since 180° magnetic arc BLDC motor is used, 120° conduction interval is applied to virtual inverter to maintain the stator current as rectangular so as to produce the constant torque. In 120° conducting interval, only two devices are in ON state. One device is from positive side switch and connected with one phase and the second device is from negative side switch and is connected with other phase. The third phase is floating. The inverter is commutated at every 60 degrees so that the rectangular line current is in phase with the back EMF. The inverter has only six switching states to avoid the short circuit at the two terminal DC side and open circuit at the motor side. Table II shows the six switching states of the inverter for forward and reverse rotation.

TABLE II
SWITCHING STATES OF VIRTUAL INVERTER

Rotor Position	Forward Rotation						ON state switches
	Hall Sensor Output			Output Phase			
	H1	H2	H3	a	b	c	
0 - 60°	1	0	0	1	0	-1	S_{a+} & S_{c-}
60 - 120°	1	0	1	1	-1	0	S_{a+} & S_{b-}
120 - 180°	0	0	1	0	-1	1	S_{c+} & S_{b-}
180 - 240°	0	1	1	-1	0	1	S_{c+} & S_{a-}
240 - 300°	0	1	0	-1	1	0	S_{b+} & S_{a-}
300 - 360°	1	1	0	0	1	-1	S_{b+} & S_{c-}

C. Generation of Gate Pulses

The virtual rectifier and the virtual inverter are fictitious stages. The modulation schemes of two stages are merged into one modulation scheme. In the virtual rectifier stage, there are six switching states to obtain the two terminal DC output and in virtual inverter stage also there are six switching states according to the hall sensor output. While combining these two stages there are 36 switching states to drive the BLDC motor. The transfer matrix has been realized as a function of input voltage and rotor position/hall sensor.

$$\begin{bmatrix} S_{Aa}(t) & S_{Ba}(t) & S_{Ca}(t) \\ S_{Ab}(t) & S_{Bb}(t) & S_{Cb}(t) \\ S_{Ac}(t) & S_{Bc}(t) & S_{Cc}(t) \end{bmatrix} = f(V_{in}, halloutput) = f(V_{min}, V_{max}, H1, H2, H3) \quad (9)$$

For example, the input phases *C* and *A* are most positive and most negative phases respectively and rotor angular position is between 0 and 60°. For the rotor angular position of 0° to 60°, the output phases *a* and *c* will be connected to the motor. The switch S_{Ca1} and S_{Ac2} are ON and other switches are OFF in this interval. The switch S_{Ca1} is the IGBT switch which carries positive current in S_{Ca} bidirectional device. The switch S_{Ac2} is the IGBT switch which carries negative current in S_{Ac} bidirectional device. Fig. 4 shows the switching states for this interval. For the change in the rotor position, only one switch will be commutated.

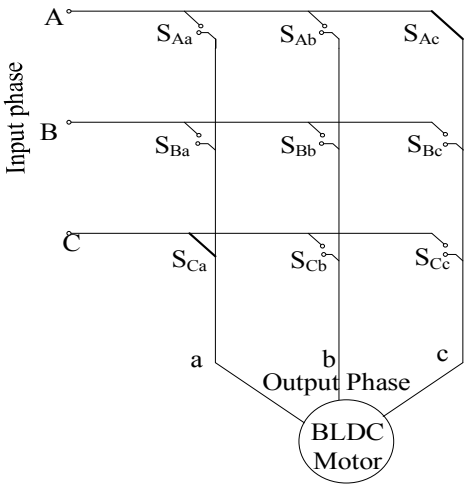

Fig. 4 Switching States of matrix converter (Input phases C and A are most positive and most negative phases respectively and rotor angular position is between 0 and 60°)

V. Closed loop control

Fig. 5 shows the overall block diagram. It consists of a current control loop that regulate the torque of the BLDC motor and a speed control loop that regulates the speed of the BLDC motor. The set speed ω* (rad/sec) and actual rotor speed ω_{actual} (rad/sec) of the motor are compared and the speed error ω_{error} is given to the speed controller. The regulation of speed is accomplished with speed controller and reference torque T_{ref} is produced. The reference current (I_{ref}) is derived from the reference torque T_{ref} used in the current control loop. Current control loop consists of reference current generator and the hysteresis current controller. The reference current generator block generates the three phase reference currents (I_{a*}, I_{b*}, I_{c*}) which are timed according to the hall sensor which is shown in Table II. These appropriate timed reference currents are in rectangular shape and in phase with the respective trapezoidal back EMF to generate the maximum unidirectional torque. The reference currents are given to the hysteresis controller. The hysteresis controller regulates the motor currents within a small band around the reference current and generates the switching pattern. The switching patterns from hysteresis controller and max-min detector are combined to generate the switching pattern for matrix converter.

A. Hysteresis Current Controller

The reference phase currents from reference current generator are compared with phase currents of the motor. From these error currents, the switching is generated depending on its relationship to the hysteresis current window. The voltage to be applied to the BLDC motor is derived by comparing the reference current to the motor phase current using the following equation

$$\begin{aligned} if(i^* - i) \geq \Delta i \quad , then\, V = V_{DC} \\ if(i^* - i) \leq \Delta i, \quad then\, V = 0 \end{aligned} \quad (10)$$

where Δi is the hysteresis band.

B. Speed Controller

The regulation of speed is achieved using speed controller. In the speed control loop the reference speed ω^* and actual speed ω_{actual} are compared in error detector and error signal is obtained. This error signal is manipulated in PI and fuzzy logic control based speed controller. The output of speed controller is reference torque T_{ref} for the current control loop.

1. PI Speed Controller

The speed regulation is accomplished in PI controller. By increasing the proportional gain of the speed controller, better tracking of speed reference is achieved and sensitivity of the controller also increases, which reduces the overshoot in speed characteristics. If the proportional gain is too high, the system will become unstable and if it too small, the settling time of the speed will be high. Better speed tracking will be obtained during transient period by increasing the proportional gain. If integral gain is too high, the output of controller will saturate and the speed error required to change the reference torque is high. This will lead to sluggish response during change in the reference speed or load disturbance. If the integral gain is too small, peak overshot will be high. An optimal value of proportional and integral gain is obtained by tunings the system using ziegler-Nichols reaction rate method and the values are 0.137 and 1 respectively. An anti-windup circuit is included to overcome the saturation in integral controller.

2. Fuzzy Logic Based Speed Controller

Fuzzy logic controllers are inherently robust to load disturbance and change in system operating conditions also they are easy to implement [9], [15], [26]. The variables involved in the antecedent part are the input variables. In this system, error and change in error are input variables. The error $e(t)$ is the difference between reference speed ω^* and actual speed ω_{actual} and the change in error $ce(t)$ is the ratio of difference between two successive sampling errors to the sampling period shown as

$$e(t) = \omega^* - \omega_{actual} \quad (11)$$

$$ce(t) = \frac{[e(t)-e(t-1)]}{T} \quad (12)$$

The input variables $e(t)$ and $ce(t)$may be positive, zero and negative which leads to seven fuzzy set values. The output variable T_{ref} may also be positive, zero and negative which leads to seven fuzzy set values. The fuzzy set values are Negative Big (NB), Negative Medium (NM), Negative Small (NS), Zero (ZE), Positive Small (PS), Positive Medium (PM) and Positive Big (PB).

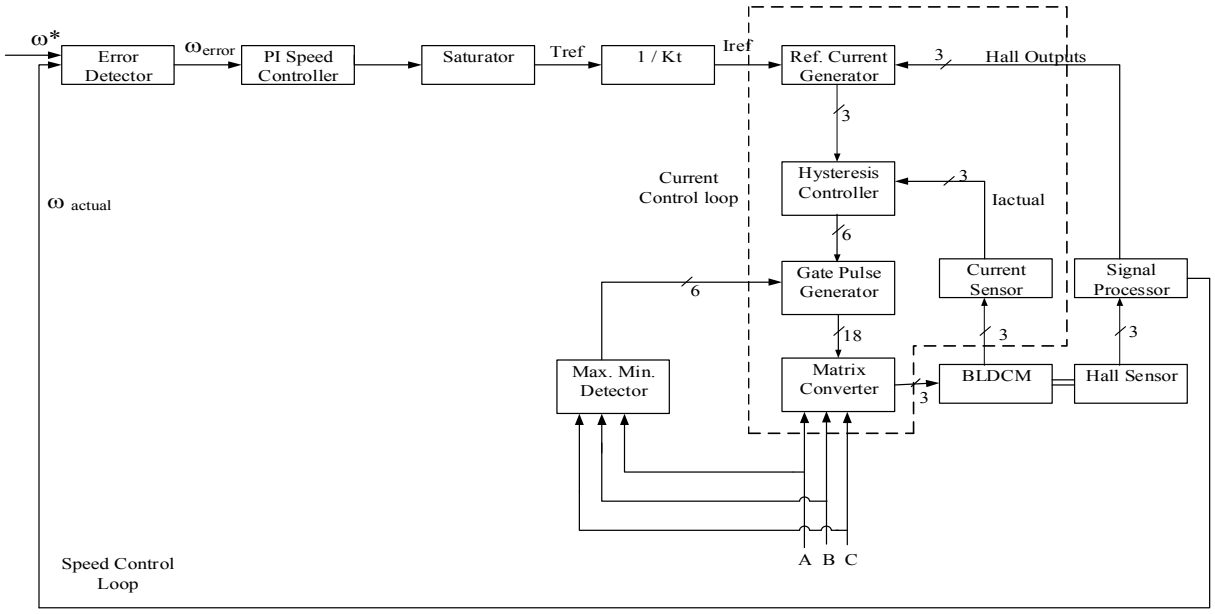

Fig. 5 Closed Loop control of MC fed BLDCM

TABLE III
RULE TABLE OF FUZZY LOGIC CONTROLLER

Change in error $ce(t)$	Error $e(t)$ NB	NM	NS	ZE	PS	PM	PB
NB	NB	NB	NB	NB	NM	NS	ZE
NM	NB	NB	NB	NM	NS	ZE	PS
NS	NB	NB	NM	NS	ZE	PS	PM
ZE	NB	NM	NS	ZE	PS	PM	PB
PS	NM	NS	ZE	PS	PM	PB	PB
PM	NS	ZE	PS	PM	PB	PB	PB
PB	ZE	PS	PM	PB	PB	PB	PB

The input and output variables are normalized between -1 and +1. With these fuzzy values, a complete rule table with 49 rules is formed as shown in Table III. The input crisp values are converted into these fuzzy values using triangular membership function in fuzzification module and given to inference engine. The triangular membership function is shown in Fig. 6. In the inference engine, min-max compositional rule is adopted and is best suited for hardware implementation since min-max comparisons alone are involved and there is no multiplication. The result of inference engine is fuzzified torque component of machine current. This fuzzy value is converted into crisp value in defuzzification module.

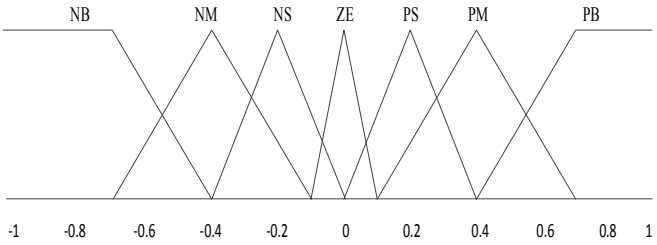

Fig. 6 Membership graph for fuzzy variables

VI. RESULTS AND DISCUSSION

A. Simulation Results

The specifications of the BLDC motor are shown in Table IV. The proposed switching algorithm is used to generate the firing pulses for 18 IGBTs in matrix converter. The input voltage of 124V is given to three phase matrix converter. In the PI speed controller based closed loop system, initially 500 RPM is set as the reference speed and operated at no load.

TABLE IV
SPECIFICATIONS OF BLDC MOTOR

continuous stall torque	2.2 Nm
torque constant	0.49 Nm/A
max speed	4600 RPM
moment of inertia	1.8/1.4 kgcm^2
per phase resistance	3.07 ohms
per phase inductance	6.57e-3H
voltage (line-line)	210 V

The speed of the motor reaches the set speed at 0.005 sec as shown in Fig. 7. During the transient period, the motor develops the rated torque of 6.6Nm to reach the set speed at the faster rate. At 0.05 sec, the reference speed of the motor is increased to 600 RPM. At 0.1 sec, the load torque of 1Nm is applied and the torque developed by the motor is shown in Fig. 8. The motor draws the required higher current from the supply to meet the requirement of the load torque. The stator current and the back EMF are shown in Figs. 9 & 10 respectively. Fig. 11 shows the input current of the matrix converter and the current is not in sinusoidal shape. Fig. 12 shows the speed characteristics of the BLDCM using FLC based speed controller for the same input. It is observed that the settling time is 0.034 sec which is less than that of PI based system. When the load of 1 Nm is applied, the reduction in speed is not noticeable whereas in PI based system, the motor regains the set speed after 0.1 sec only. Hence, it is proved that the FLC based system performs well in both steady state and dynamic conditions.

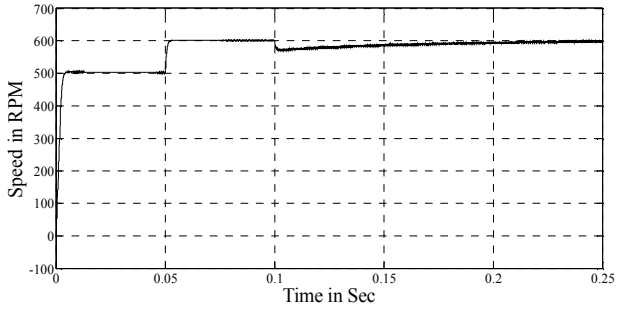

Fig. 7 Speed Characteristics of BLDCM using PI controller

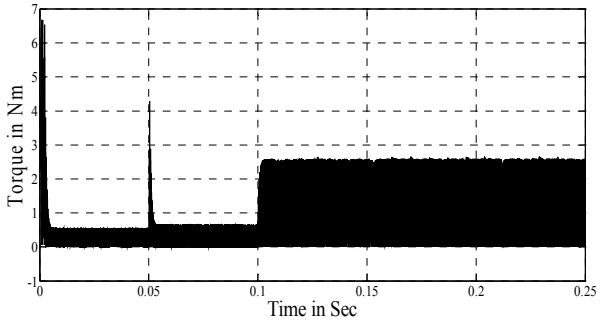

Fig. 8 Torque Characteristics of BLDCM

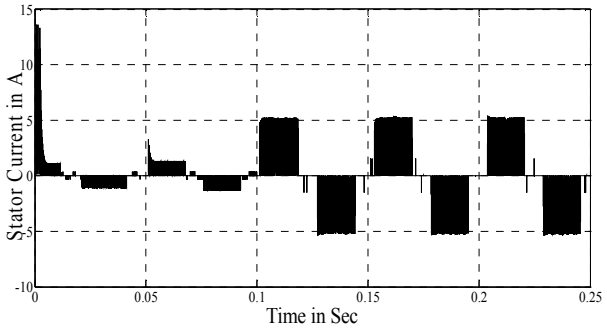

Fig. 9 Stator Current of BLDCM

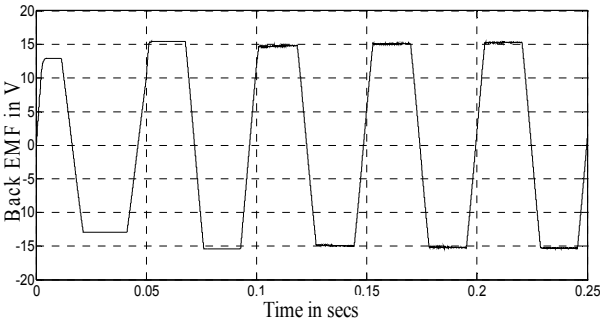

Fig. 10 Trapezoidal Back EMF of BLDCM

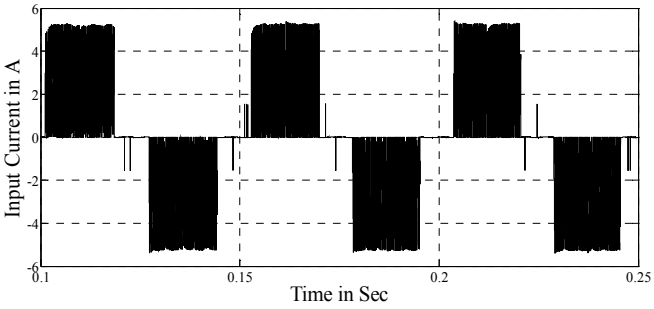

Fig. 11 Input phase current of Matrix Converter

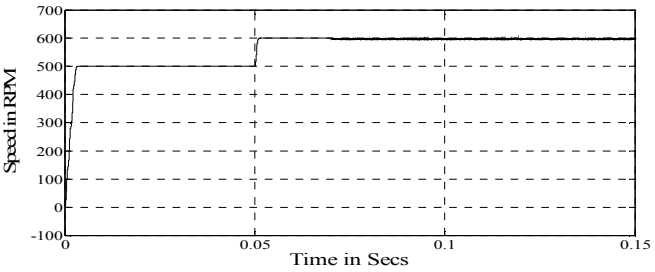

Fig. 12 Speed characteristics of BLDCM using FLC

B. Hardware Results

A three phase to three phase matrix converter was designed using 18 IGBTs. The common emitter bidirectional switch consists of two diodes and two IGBTs which are connected in anti parallel. A three phase, 440V, 50Hz supply is given to MC through a three phase auto transformer. Initially the max-min voltages of input three phase supply are sensed using the circuit as shown in Fig. 13 and are given to FPGA SPARTAN 3Ekit. The position of the rotor is sensed using the hall sensor. The output of the three hall sensors areas shown in Fig. 14 and these signals are given to SPARTAN kit. The 18 gate pulses for IGBTs are generated using controller. The waveforms are captured using WT1800 Yokogawa 6 channel power analyzer as shown in Fig. 15. The switching frequency was set as 10 KHz. The input side filter inductor and capacitor were chosen to be 120μH and 50μF respectively. Fig. 16 shows the input phase voltage and current to the matrix converter and it is observed that the input voltage and current are in phase but the input current is in rectangular shape. Figs. 17 and 18 show the stator current and voltage respectively. Fig 19 shows the

hardware setup of Matrix converter fed BLDC Motor using FPGA processor.

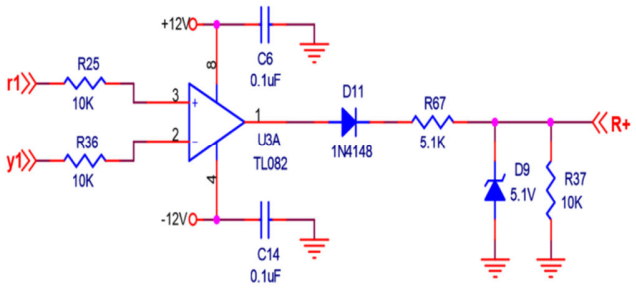

Fig. 13 Circuit to sense max-min voltage (R^+)

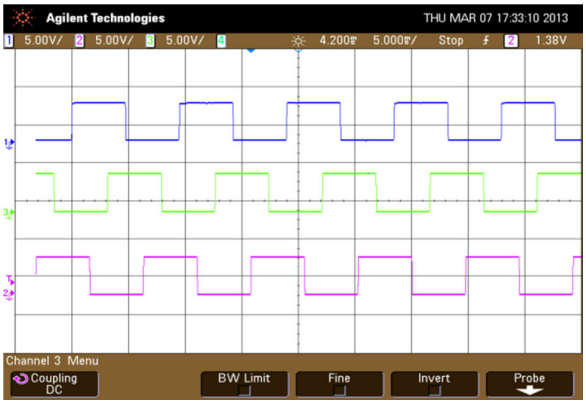

Fig. 14 Output of hall sensors

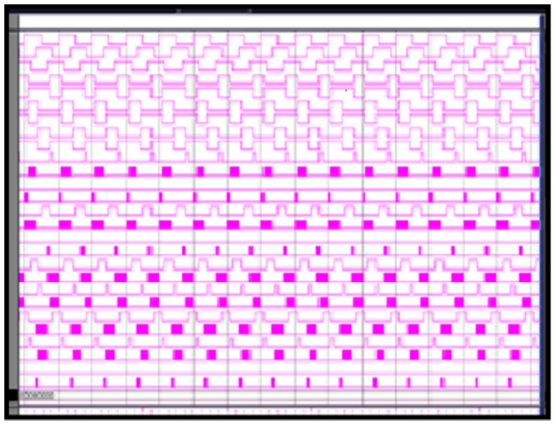

Fig 15 The switching patterns for power devices

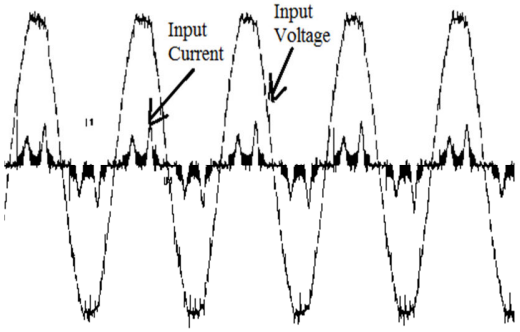

Fig. 16 Input phase voltage and current

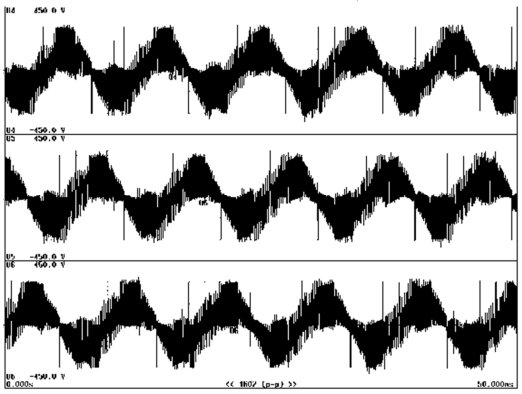

Fig. 17 Stator current

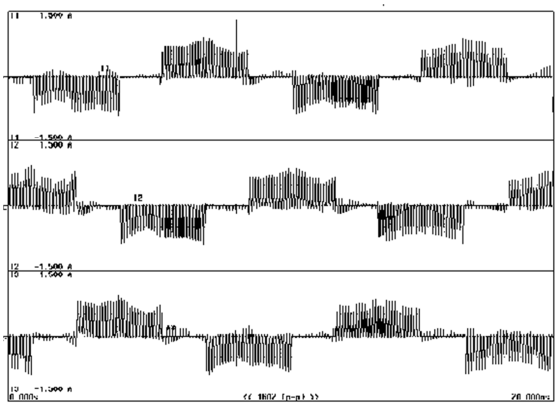

Fig. 18 Stator voltage

Fig. 19 Experimental Setup of matrix converter fed BLDC Motor

VII. Conclusion

This paper has presented a set of control methodologies to control the three phase to three phase matrix converter fed BLDC motor. The proposed algorithm allowed the control of speed characteristics of BLDC motor in a flexible manner. Two sets of experimental setup were studied. In the first case, a separate PI controller and a hysteresis controller were designed to study the performance of speed and torque control. In the second case, the same was repeated with the FLC in the place of the PI controller. The outcome of the research is that the FLC based system exhibits better performance as compared to the PI based system. Experimental results validate the validity of the proposed

control schemes. This work can be extended further by incorporating braking and regenerative operations for four quadrant drive and torque characteristics can be improved by adopting any one of the torque ripple minimization technique. Also by replacing the direct matrix converter by indirect matrix converter, the sinusoidal input current may be obtained.

REFERENCES

[1] Jiancheng Fang, Xinxiu Zhou, Gang Liu, "Instantaneous Torque Control of Small Inductance Brushless DC Motor', *IEEE Transactions on Power Electronics*, Vol. 27, No.12, pp. 4952-4964, Dec. 2012.

[2] F. Aghili, "Fault Tolerant Torque control of BLDC motors" , *IEEE Transactions on Power Electronics*, Vol. 26, No.2, pp. 355-363, Nov. 2011.

[3] Y. S. Lai, Y. S. Lin, "A unified Approach to Zero crossing point detection of back EMF for Brushless DC motor drives without current and hall Sensors" *, IEEE Transactions on Power Electronics*, Vol. 26, No.6, pp. 1704-1713, June. 2011.

[4] Viswanathan, Jeevanantham, "A Novel current controlled Space vector modulation based Control Scheme for Reducing Torque Ripple in Brushless DC Drives", *International Journal of Computer applications*, Vol.28, no.2, pp.25-31, August. 2011.

[5] Sheeba Jose, Paranjothi, Jawahar Senthil Kumar, "Digital control Strategy for Four quadrant Operation of Three Phase BLDC Motor with load variations", *IEEE Transactions on Industrial Informatics*, vol.9, no.2, pp. 974-982, May. 2013.

[6] Bharani Kumar, Nirmal Kumar, "Performance Analysis of wind Turbine –driven permanent magnet generator with matrix converter", *Turk J ElecEng & Comp Sci*, vol. 20, no.3, pp.299-317, 2012.

[7] Tiangui Jiang, Bozhou, Chumei Hong, Mingmingshi, "New Modulation Scheme for matrix converter driving BLDC Motor", *International Conference on Electrical machines and systems*, Oct. 2008, pp.1445-1450.

[8] J. Karpagam, Dr. A. N. Kumar, V. Kumar, "Comparison of Modulation Techniques for Matrix Converter", IACSIT *Int J of Engg & Tech*, vol.2,No.2, pp189-195, April. 2010.

[9] Chitra Venugopal, K. S. Ravi Chandran, R. Varadharajan, "Fuzzy logic Based Matrix converter for the speed control of Induction motor", *Journal of Electrical Engineering: Theory and Application*, Vol. 1, issue3, pp. 151-157, June. 2010.

[10] Vinod Kumar, Ramesh Chand Bansal and Raghuveer Raj Joshi, "Experimental realization of Matrix Converter based Induction Motor Drive under Various Abnormal Voltage Conditions*", International Journal of Control, Automation and Systems*, Vol. 6, No.5, pp. 670-676, October, 2008.

[11] Djahbar, B. Mazari, and M. Latroch, "Control Strategy of Three-Phase Matrix Converter Fed Induction Motor Drive System" *IEE Pulsed Power Symposium*, Vol. 11, Sep. 2005, pp. 1-6.

[12] S. Bala, G. Venkataraman, "Matrix Converter BLDC Drive using reverse Blocking IGBTs", *Proc IEEE APEC* March. 2006, pp. 660-666.

[13] Xiaoyan Huang, Andrew Goodman, Gerata, Youtong Fang, Quifen Lu, "A Single Sided Matrix Converter for a brushless DC motor in Aero Space Application", *IEEE Transaction on Industrial Electronics*, vol.59, no.9, 3542-3552, Sep. 2012.

[14] P. W. Wheeler, Rodriguez, J. C. Clare, L. Empringham and A. Weinstein, "Matrix Converters: A technology review*", IEEE Transaction on Industrial Electronics*, vol 49, No2, pp. 276–288, April. 2002.

[15] K. B. Lee, F. Blaaberg, "Sensorless DTC-SVM for Induction Motor drive using parameter estimation strategies", *IEEE Transaction on Industrial Electronics*, vol.55, 512-521, Feb. 2008.

[16] Rodriguez, Rivera Macro, J. W. Kolar, P. W. Wheeler, "A Review of control and modulation methods for matrix converters", *IEEE Transaction on Industrial Electronics*, vol 59, 58-70, Jan.2012.

[17] Kolar J W, Friedi Thomas, Wheeler PW, "Review of three phase PWM AC-AC converter topologies", *IEEE Transaction on Industrial Electronics,* vol 58, 4988-5005, Nov. 2011.

[18] P. Pillay and R. Krishnan, "Modeling, simulation and analysis of permanent-magnet motor drives, part-II: the brushless DC motor drives", *IEEE Transaction on Industrial Applications*, vol.25, 274-279, Apr. 1989.

[19] Byoung-KuK Lee and Mehrdad, "Advanced simulation Model for Brushless DC motor drives", *Electric Power Components and systems*, vol. 31:9, 841-868,2003.

[20] Goh Teck Chiang, Jun-ichi-Itoh, "Comparison of Two Overmodulation strategies in an Indirect Matrix Converters", *IEEE Transaction on Industrial Electronics,* vol.60, No.1, 43-53, Jan. 2013.

[21] Brahmin Metidji, Nabil Taib, Toufik Rekioua, Seddik Bacha, "Phase Current Reconstruction using a Single Sensor of Three phase AC motors fed by SVM controlled Direct matrix Converter", *IEEE Transaction on Industrial Electronics*, vol.60,No.12,5497-5504, Dec. 2013.

[22] Tae-Won Chun, Quang-Vinh Tran, Hong-Hee Lee, Heung-Geun Hong-Hee Lee, Heung-Geun Kim, "Sensorless control of BLDC Motor Drive for an automative Fuel Pump using a Hysteresis Comparator", *IEEE Transaction on Power Electronics*, vol.29, No.3, pp 1382-1391, March. 2014.

[23] Dan Xiao, M. F. Rahman, "Sensorless Direct torque and flux Controlled IPM Synchronous machine Fed By Matrix Converter over a Wide Speed range" *, IEEE Transaction on Industrial Informatics*, Vol.9 No.4, 1855 – 1866, Nov. 2013.

[24] Jiacheng Wang, Bin Wu, Dewei Xu, Zargari, N.R., "Phase Shifting transformer fed Multimodular matrix converter operated by a new modulation strategy", *IEEE Transaction on Industrial Electronics*", vol.60, no.10, 4329-4338, Oct. 2013.

[25] Chin-long Cham, Zahurin Bin Samad, "Brushless DC Motor Electromagnetic Torque Estimation with Single Phase Current Sensing", *J Electrical Engineering & Technology*, Vol.9, No.3,866-872, May. 2014.

[26] P. Subha Karuvelam,, M. Rajaram, "Control of Speed and Torque in Matrix Converter fed BLDC Motor using FPGA Controller", *International Journal of Power and Energy Systems*, vol.34, no.3, pp. 99-108, 2014.